Growth of Carbon Nanotubes on HfO_2 towards Highly Sensitive Nano-Sensors

Takashi Uchino, Greg N. Ayre[1], David C. Smith[1], John L. Hutchison[2], C. H. de Groot, and Peter Ashburn

School of Electronics and Computer Science, University of Southampton, Southampton SO17 1BJ, United Kingdom
[1]*School of Physics and Astronomy, University of Southampton, Southampton SO17 1BJ, United Kingdom*
[2]*Department of Materials, University of Oxford, Parks Road, Oxford, OX1 3PH, United Kingdom*

Received October 1, 2009; accepted December 2, 2009; published online April 20, 2010

Carbon nanotube (CNT) growth on HfO_2 is reported for the first time. The process uses a combination of Ge and Fe nanoparticles and achieves an increase in CNT density from 0.15 to 6.2 μm length/μm^2 compared with Fe nanoparticles alone. The synthesized CNTs are assessed by the fabrication of back-gate CNT field-effect transistors with Al source/drain contacts for nano-sensor applications. The devices exhibit excellent p-type behavior with an I_{on}/I_{off} ratio of 10^5 and a steep sub-threshold slope of 130 mV/dec.

DOI: 10.1143/JJAP.49.04DN11

1. Introduction

Recently, carbon nanotube field-effect transistors (CNTFETs) are gaining much attention for sensor applications,[1–3] especially bio-sensing because they offer the prospect of real-time, label-free sensing for point-of-care diagnosis. The main advantage of CNTFETs for these applications is a high sensitivity due to the large surface to volume ratio of a CNT. For bio-sensing, a back gate structure is often used because it is necessary to expose CNTs to the biomolecules. A back gate structure also delivers a cheap and simple fabrication process compared with a top gate structure, which is advantageous for point-of-care healthcare applications. Sensitivity is a key issue in biosensors and a high I_{on}/I_{off} ratio is desirable in achieving this goal and can be achieved by the introduction of high-κ gate dielectrics. Among a variety of high-κ materials, HfO_2 is considered as one of the most promising candidates due to a high dielectric constant of around 25.[4] CNTFETs with a HfO_2 gate dielectric have also recently been researched for application in high-speed nonvolatile memory and a strong hysteresis effect has been reported.[5] The memory effect of this device is attributed to the oxygen vacancy states in HfO_2 rather than the adsorption of molecules such as water. It is very difficult to place CNTs onto HfO_2 using dispersion techniques due to the hydrophobic nature of HfO_2.[6] Equally, chemical vapor deposition (CVD) of CNTs on HfO_2 appears to be very hard and to our knowledge no work has been reported on this topic to date in spite of the fact that CVD process would be more compatible with mainstream silicon technology.

In this paper, a CNT growth process on HfO_2 is reported for the first time. The novel growth process uses a combination of Ge and Fe nanoparticles to achieve a dramatic increase in CNT yield compared with the use of Fe nanoparticles alone. The synthesized CNTs are applied to back-gate CNTFETs with Al source/drain (S/D) contacts for nano-sensor devices. After H_2 anneal at 400 °C, the devices exhibit p-type behavior with an I_{on}/I_{off} ratio of 10^5 and a steep sub-threshold slope of 130 mV/dec.

2. Experimental Methods

A p^+ Si substrate (0.005 Ω·cm) was employed as a back gate. After a standard cleaning process, a gate dielectric stack of SiO_2/HfO_2 (45/10 nm) was formed. The interfacial SiO_2 layer was thermally grown and the HfO_2 layer was grown by atomic-layer deposition. A 30-nm-thick-SiO_2 layer was then deposited by plasma enhanced chemical vapor deposition (PECVD) on the HfO_2 layer and densified at 950 °C. The top SiO_2 layer was then implanted with 5×10^{15} cm^{-2}, 20 keV Ge and annealed in N_2 at 600 °C for 40 min to create Ge nanoparticles. The top SiO_2 layer was then removed using a HF vapor etch to expose the Ge nanoparticles on the HfO_2 layer. Then the substrate was dipped in ferric nitrate solution for 1 min and rinsed with hexane. The CNT growth was carried out using CVD in a hot-wall reactor at atmospheric pressure. CNTs were grown at 850 °C for 20 min using a mixture of methane (1000 sccm) and H_2 (300 sccm) immediately after a pre-anneal in H_2 (1000 sccm) at 900 °C. For comparison, CNT growth on HfO_2 using Fe nanoparticles only was also carried out.

Back gate CNTFETs were fabricated with Al S/D contacts for nano-sensor devices. Al was deposited by sputtering and the S/D electrodes were formed using direct write optical lithography and lift-off. The use of Al instead of the more common Pd can both reduce the cost and improve the yield, as Pd has poor adhesion to HfO_2. The gap between the S/D electrodes was 2.0 μm and the width was 5.0 μm. After Al patterning, the devices were annealed in H_2 at 400 °C for 30 min.

The synthesized CNTs were observed by means of field emission scanning electron microscope (FE-SEM) and high resolution transmission electron microscope (HRTEM). TEM sample preparation consisted of scraping the sample surface with a surgical blade and transference onto a carbon-coated Cu grid. The area densities of CNTs were evaluated using FE-SEM images and ImageJ[7] was used to determine the total contour length of CNTs. Ten SEM images with a typical size of 15 μm^2 were taken from the same sample and used for quantitative analysis, with overlapping regions being discarded. Raman spectra were obtained using a micro-Raman system with He–Ne ($\lambda = 632.8$ nm) laser excitation with power of 12 mW.

3. Results and Discussion

The Ge nanoparticles were evaluated by means of atomic force microscopy (AFM). These results showed a high particle density of 460 ± 30 particles/μm^2, with an average particle height of 2.1 ± 0.8 nm. This result agrees well with previous results by Min *et al.*[8] who reported the formation of Ge nanocrystals, by a similar process, with an average size of 1.9 ± 0.8 nm. Figure 1 shows FE-SEM images after CNT growth for samples using Fe nano-particles only (a) and a combined Fe/Ge nanoparticles (b). For Fe nano-

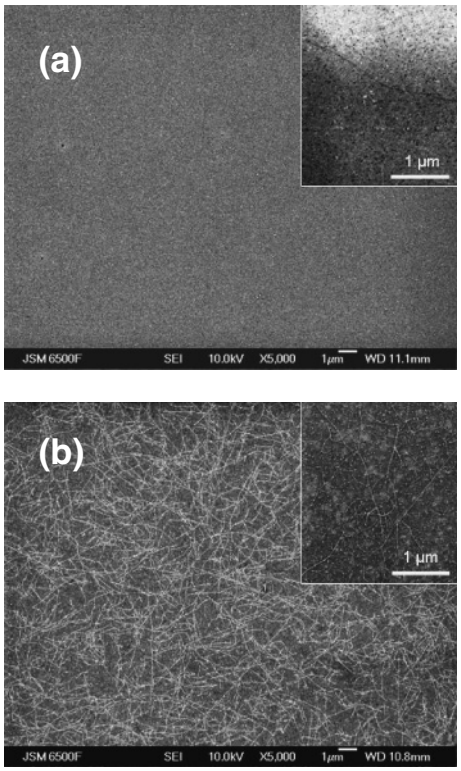

Fig. 1. FE-SEM images after CNT growth on HfO_2 substrates using Fe nanoparticles only (a) and a combination of Ge and Fe nanoparticles (b). CNT area densities are 0.15 and 6.2 μm length/μm^2 respectively.

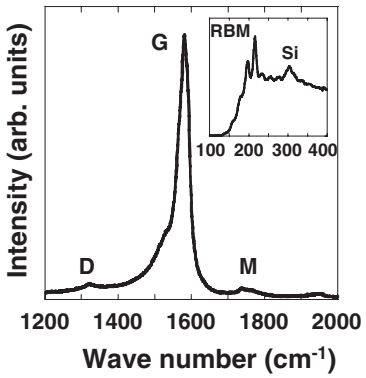

Fig. 2. Raman spectra of CNTs grown from a combination of Ge and Fe nanoparticles on HfO_2 substrate. The inset shows radial breathing mode (RBM), indicating that SWNTs are present.

particles only, very few CNTs are present and only isolated CNTs are occasionally seen as shown in inset of Fig. 1(a). The area density of CNTs was estimated by the average total length of CNTs (μm) per unit area (μm^2) and found to be 0.15 μm length/μm^2. In contrast, the presence of the Ge nanoparticles dramatically enhances CNT growth, giving an area density of 6.2 μm length/μm^2. These results indicate that the presence of Ge nanoparticles dramatically increases the area density of CNTs. Furthermore, the results suggest that selective CNT growth may possible by using photo resist mask patterns during the Ge ion implantation.

The CNTs grown from the combined Fe/Ge nanoparticles were characterized by micro Raman spectroscopy and the results are shown in Fig. 2. All samples clearly showed the radial breathing mode (RBM) and M-band, indicating that

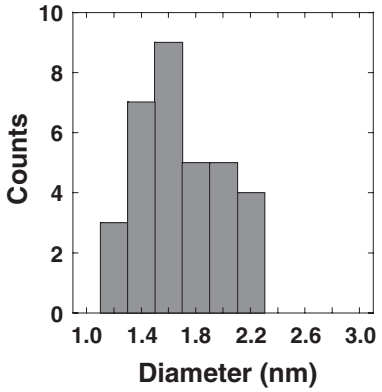

Fig. 3. A histogram of the diameter distribution of SWNTs obtained by HRTEM.

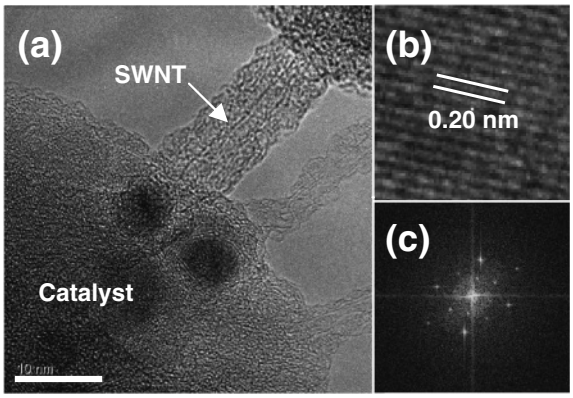

Fig. 4. (a) HRTEM image of SWNTs and nanoparticles. (b) High magnification of the area in the nanoparticle. (c) The corresponding fast Fourier transform image of the nanoparticle.

single-walled CNTs (SWNTs) are present. The Raman intensity ratio (I_D/I_G) of D-band to G-band was less than 0.1, indicating that synthesized SWNTs have a low defect density. The diameter distribution of SWNTs is estimated at 1.5–2.0 nm from the RBM peaks, though larger diameter SWNTs may be present due to the cut-off of Raman notch filter.

Figure 3 shows the diameter distribution of the SWNTs which was obtained from fifteen HRTEM images. The mean diameter of 1.7 ± 0.5 nm is in good agreement with the Raman estimate.

The origin of the SWNTs was investigated by HRTEM and the resulting HRTEM images and corresponding electron diffraction patterns are shown in Fig. 4. The HRTEM images show the presence of at least two distinct nanoparticles with a diameter around 6 nm and SWNTs appear to originate from these nanoparticles. The SWNTs are wrapped with amorphous carbon layers, which are probably due to the long growth time of 20 min. The undesirable amorphous carbon coating could be avoided if the growth time was reduced to around 5 min.[9] Raman measurements show that most of the SWNTs have a low intensity of D-band peak which indicates the presence of both a small amount of amorphous carbon and of defects. To investigate the nature of the nanoparticles, TEM, operating at 300 kV, with energy dispersive X-ray analysis (EDX) was carried out on the nanoparticle and the spectra from the

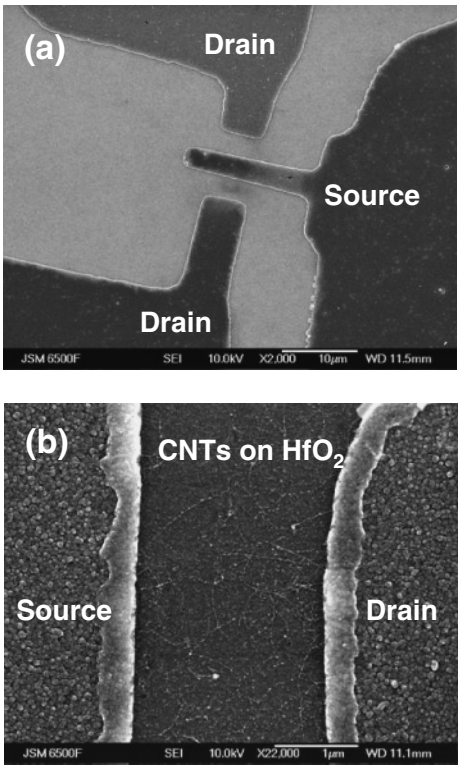

Fig. 5. (a) Low magnification FE-SEM image of Al contacted CNTFETs on HfO_2. (b) The CNT distribution between source and drain contacts.

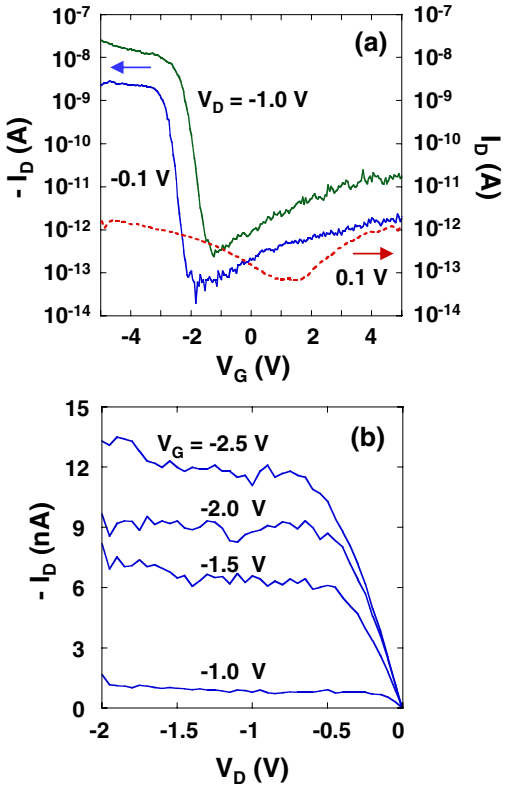

Fig. 6. (Color online) *I–V* characteristics of an Al contacted CNTFET with channel length $L_G = 2.0\,\mu m$. (a) Subthreshold characteristics before and after H_2 anneal. The broken line shows the data for $V_D = +0.1$ V before H_2 anneal. The solid lines show the data for $V_D = -0.1$ and -1.0 V after H_2 anneal. (b) Output characteristics for $V_G = -1.0$, -1.5, -2.0, -2.5 V after H_2 anneal.

nanoparticles indicate that the atomic ratio of Fe/Ge is 3.2. As the nanoparticle is surrounded and sat on substrate material into which Ge was implanted, it is likely that the nanoparticle is richer in Fe relative to Ge than this ratio implies. A lattice image of the nanoparticle was also taken and is shown in Fig. 4(b). The measured lattice spacing is 0.20 nm and the corresponding fast Fourier transform pattern [Fig. 4(c)] gives a lattice constant for the nanoparticle of 0.28 nm which is in reasonable agreement with the lattice constant of Fe ($a = 0.29$ nm), and quite different from the lattice constant of FeGe ($a = 0.47$ nm).[10] In our previous work on the growth of CNTs on Si using Ge nanostructures, we found that the growth of CNTs was possible from Ge nanoparticles without the presence of a metal catalyst.[11–13] However, in this work, the results in Fig. 4 indicate that CNTs were grown from the Fe nanoparticles, rather than the Ge nanoparticles. In interpreting these results, it should also be noted that Fig. 1(a) shows little CNT growth when only Fe nanoparticles are present. Thus the improvement of CNT area density when Ge nanoparticles are combined with Fe nanoparticles can be attributed to a reduction of interactions between the Fe nanoparticles and the HfO_2 layer due to the presence of the Ge nanoparticles.

Figure 5 shows FE-SEM images of a back gate CNTFET with a SiO_2/HfO_2 gate dielectric and Al S/D contacts. The SWNTs bridge the 2.0 μm gap between the Al S/D electrodes, giving a channel length of greater than 2 μm. The back gate structure has been used for compatibility with nano-sensor fabrication. We have successfully fabricated in total more than 80 functional devices with p-type behavior. 69% of the devices show semiconducting behavior and 31% of them show metallic behavior.

Figure 6 shows sub-threshold and output characteristics for one of the best CNTFETs. The characteristics were measured in ambient air and it can be clearly seen that the devices are converted from weak ambipolar to p-type behavior after the H_2 anneal. The sub-threshold characteristics show an excellent I_{on}/I_{off} ratio of 10^5 and a reasonably steep sub-threshold slope of 130 mV/dec. The achieved I_{on}/I_{off} ratio of 10^5 at $V_{CC} = 1.5$ V is much higher than the previously reported value of 10^3 for Al contacted p-type CNTFETs.[14] However it is equivalent to or higher than reported values for Al contacted n-type CNTFETs.[15–18] The behavior in the positive gate voltage region is mainly attributed to gate leakage current rather than the ambipolar conduction, because the leakage current level is very close to the gate current. The output characteristic shows linear characteristics at small drain voltages ($V_D > -0.5$ V) and good saturation at large drain voltages ($V_D < -0.5$ V). The steep values of sub-threshold slope and linear output characteristics below saturation suggest that the Al-CNT contact has a low Schottky barrier height. This result is rather surprising, as earlier research on CNTFETs with Al S/D contacts has either shown weak p-type behavior[14] or strong n-type behavior.[15–18] Work is currently underway to investigate the physical explanation for these very promising electrical results, however it is clear that the work function of Al is unaffected after H_2 anneal[19,20] in contrast to the behavior of Pd.[21] It can therefore be concluded the p-type behavior is caused by the modification of the electronic structure of the CNTs, possibly during the H_2 anneal.

4. Conclusions

We have developed a novel CNT growth process on HfO_2 using a combination of Fe and Ge nanoparticles. The presence of the Ge nanoparticles significantly increases CNT area density. The synthesized CNTs were successfully applied to fabricate back gate CNTFETs with Al S/D contacts. The CNTFETs show p-type behavior with an excellent I_{on}/I_{off} ratio of 10^5 and a steep sub-threshold slope of 130 mV/dec after H_2 anneal.

Acknowledgement

The authors acknowledge EPSRC for supporting this work.

1) U. Schwalke and L. Rispal: ECS Trans. **13** (2008) No. 22, 39.
2) J. Kong, N. Franklin, C. Zhou, S. Peng, J. Cho, and H. Dai: Science **287** (2000) 622.
3) P. Collins, K. Bradley, M. Ishigami, and A. Zettl: Science **287** (2000) 1801.
4) J. Locquet, C. Marchiori, M. Sousa, J. Fompeyrine, and J. Seo: J. Appl. Phys. **100** (2006) 051610.
5) M. Rinkio, A. Johansson, G. S. Paraoanu, and P. Torma: Nano Lett. **9** (2009) 643.
6) J. Hannon, A. Afzari, Ch. Klinke, and Ph. Avouris: Langmuir **21** (2005) 8569.
7) ImageJ program [http://rsb.info.nih.gov/ij/].
8) K. Min, K. Shcheglov, C. Yang, H. Atwater, M. Brongersma, and A. Polman: Appl. Phys. Lett. **68** (1996) 2511.
9) C. Yeh, M. Chen, J. Gan, J. Hwang, C. Lin, T. Chao, and Y. Cheng: Nanotechnology **18** (2007) 145613.
10) M. Richardson: Acta Chem. Scand. **21** (1967) 2305.
11) T. Uchino, K. Bourdakos, C. H. Groot, P. Ashburn, M. Kiziroglou, G. Dilliway, and D. C. Smith: Appl. Phys. Lett. **86** (2005) 233110.
12) T. Uchino, K. Bourdakos, C. H. Groot, P. Ashburn, S. Wang, M. Kiziroglou, G. Dilliway, and D. C. Smith: Proc. IEEE Conf. Nanotechnology, 2005, WE-PS3-4.
13) T. Uchino, G. Ayre, D. C. Smith, J. L. Hutchison, C. H. Groot, and P. Ashburn: J. Electrochem. Soc. **156** (2009) K144.
14) Z. Chen, J. Appenzeller, J. Knoch, Y. Lin, and Ph. Avouris: Nano Lett. **5** (2005) 1497.
15) Y. Hu, K. Yao, S. Wang, Z. Zhang, X. Liang, Q. Chen, L. Peng, Y. Yao, J. Zhang, W. Zhou, and Y. Li: Appl. Phys. Lett. **90** (2007) 223116.
16) A. Javey, Q. Wang, W. Kim, and H. Dai: IEDM Tech. Dig., 2003, p. 741.
17) M. Yang, K. Teo, W. Milne, and D. Hasko: Appl. Phys. Lett. **87** (2005) 253116.
18) C. Chen, D. Xu, E. Kong, and Y. Zhang: IEEE Electron Device Lett. **27** (2006) 852.
19) K. Chino: Solid-State Electron. **16** (1973) 119.
20) S. Okuyama, K. Okuyama, N. Takinami, K. Matsushita, and Y. Kumagai: Jpn. J. Appl. Phys. **35** (1996) 2266.
21) A. Javey, J. Guo, Q. Wang, M. Lundstrom, and H. Dai: Nature **424** (2003) 654.